Journal of Anatomy

J. Anat. (2010) **217**, pp705–714 doi: 10.1111/j.1469-7580.2010.01306.x

Human microvascular lymphatic and blood endothelial cells produce fibrillin: deposition patterns and quantitative analysis

Antonella Rossi,[1*] Erica Gabbrielli,[1*] Marilisa Villano,[1] Mario Messina,[2] Francesco Ferrara[2] and Elisabetta Weber[1]

[1]*Molecular Medicine Section, Department of Neuroscience, University of Siena, Siena, Italy*
[2]*Department of Pediatrics, Obstetrics and Reproductive Medicine, Pediatric Surgery Section, University of Siena, Siena, Italy*

Abstract

Fibrillin microfibrils constitute a scaffold for elastin deposition in the wall of arteries and form the anchoring filaments that connect the lymphatic endothelium to surrounding elastic fibers. We previously reported that fibrillin is deposited in a honeycomb pattern in bovine arterial endothelial cells, which also deposit microfibril-associated glycoprotein (MAGP)-1, whereas thoracic duct endothelial cells form an irregular web. The present immunohistochemical study was designed to verify whether lymphatic and blood human dermal microvascular endothelial cells (HDMECs) isolated from human foreskin by the sequential use of a pan-endothelial marker, CD31, and the lymphatic specific marker, D2-40, deposit fibrillin and MAGP-1. In both cell types, fibrillin and MAGP-1 co-localized and were deposited with different patterns of increasing complexity co-existing in the same culture. Fibrillin microfibrils formed a wide-mesh honeycomb leaving fibrillin-free spaces that were gradually filled. This modality of fibrillin deposition, similar to that of bovine large artery endothelial cells, was basically the same in blood and lymphatic HDMECs. In some lymphatic HDMECs, fibrillin was initially deposited as uniformly scattered short fibrillin strands probably as a result of anchoring filaments carried over from the vessels of origin. Our findings show that blood and lymphatic endothelial cells participate in fibrillin deposition in human skin.

Key words D2-40; fibrillin; immunohistochemistry; lymphatic vessels; microfibril-associated glycoprotein-1; microvascular endothelial cells.

Introduction

Microvessels, including arterioles, capillaries and venules, represent a functionally crucial part of the cardiovascular tree in regulating blood–tissue exchanges and tissue perfusion. Although blood microcirculation has been the object of extensive studies, lymphatic initial vessels have, until the last decade, represented a problem because of the difficulty of recognizing them in histological sections. The discovery of specific lymphatic markers, which allow their positive identification even when they are completely collapsed, as they often are, and of specific growth factors, has raised great interest in this long-neglected field (Scavelli et al. 2004; Jurisic & Detmar, 2009).

Among the reasons to extend basic knowledge on how blood and lymphatic vessels function, there is an increasing need in tissue-engineered vessels that may be used to replace small caliber arteries and surgically interrupted lymphatics. However, the mechanical properties of the implant, in particular the elastic recoil and burst strength, greatly depend on matrix proteins. The relevance of precoating scaffolds with matrix proteins, including fibrillin, has been recently highlighted by Stephan et al. (2006). The present study was designed to bring new insights into the deposition of a key molecule in the organization of elastic fibers, fibrillin, by blood and lymphatic endothelial cells (ECs).

Fibrillins are large (approximately 350 kDa) cysteine-rich glycoproteins of the extracellular matrix, which make up the major structural components of 10–12-nm microfibrils with a 'bead on a string' appearance (Sakai et al. 1986) that more commonly occur in association with elastin but have also been found as anchoring proteins in non-elastic tissues subjected to mechanical stress, like the ciliary zonule of the eye (Wagenseil & Mecham, 2007). In elastic tissues, fibrillin

Correspondence
Prof. Elisabetta Weber, Dipartimento di Neuroscienze, Sezione di Medicina Molecolare, Università di Siena, Via Aldo Moro, I 53100 Siena, Italy. T: 0039 0577 234083; F: 0039 0577 234191;
E: weber@unisi.it
**These authors contributed equally to this work.*

Accepted for publication *10 September 2010*
Article published online *11 October 2010*

is thought to play a pivotal role in elastin deposition: during development, fibrillin-1 and fibrillin-2 form a scaffold for the initial assembly of elastic fibers and, during postnatal life, fibrillin-1 imparts force-bearing structural support to the adult tissue (Ramirez, 2000; Carta et al. 2006). Fibrillin-1 knock-out mice die neonatally due to failure of elastic tissues that are normally subjected to stretching and expansile forces, like the aorta, diaphragm and lungs (Carta et al. 2006). In addition to this 'structural' function of support, fibrillin has an 'instructive' role due to its capability to sequester in the extracellular matrix important signaling molecules like transforming growth factor β and bone morphogenetic protein, which regulate matrix formation and remodeling (Ramirez & Sakai, 2010).

Several molecules have been shown to associate with fibrillin, among them microfibril-associated glycoprotein (MAGP)-1 and MAGP-2. MAGP-1 is a major structural component of microfibrils. It is a small glycoprotein of 31 kDa, which has been shown to reside on microfibril beads (Henderson et al. 1996); its N-terminus may also bind the C-terminus of tropoelastin (Brown-Augsburger et al. 1994, 1996). It co-localizes with virtually all fibrillin-1-containing microfibrils. MAGP-2, the expression of which peaks at elastic fiber onset during development and has recently been shown to stimulate elastic fiber assembly (Lemaire et al. 2007), has a more restricted tissue distribution in postnatal life (Gibson et al. 1998).

Fibrillin microfibrils are present in the wall of arteries and lymphatic vessels. The importance of fibrillin-1 in the structural organization of elastic arteries is highlighted by Marfan syndrome in which a mutation of the fibrillin-1 encoding gene on chromosome 15 causes severe cardiovascular defects including aortic root dilatation and a propensity to aortic dissection (Lee et al. 1991; Robinson et al. 2006). Blood capillaries, with the exception of sinusoids (Dubuisson et al. 2001), are not surrounded by fibrillin and are not associated with perivascular elastin (Gerli et al. 1990; Ryan, 2009).

As to lymphatic vessels, fibrillin has been found in the microfibrils of anchoring filaments of human skin initial lymphatic vessels (Solito et al. 1997) that connect the lymphatic endothelium to surrounding elastic fibers (Gerli et al. 1990). The connection of skin lymphatics with elastin fibers is important in maintaining their physiological role in this peculiar district and the destruction of elastin leads to lymphatic dysfunction (Ryan, 2009).

The anchoring filaments of lymphatic vessels have long been thought to simply pull apart interendothelial junctions in edema favoring interstitial fluid drainage and lymph formation (Casley-Smith, 1980). Based on the immunohistochemical demonstration of the association of fibrillin with focal adhesion molecules in initial lymphatic vessels and experimental data on stretched thoracic duct and stretched lymphatic EC cultures, we have, however, recently postulated that they may operate a mechanotransduction of mechanical signals from the extracellular matrix in cytoskeletal rearrangements and biochemical signals inside the cell (Rossi et al. 2007) to adapt lymph formation to the physiologic requirements of the surrounding interstitium.

In-vitro studies have shown that a variety of cell types deposit fibrillin in the extracellular matrix: fibroblasts, particularly those isolated from bovine nuchal ligament (Sakai et al. 1986; Kielty & Shuttleworth, 1993), aortic smooth muscle cells (Kielty & Shuttleworth, 1993), osteoblasts (Kitahama et al. 2000), chondroblasts (Sakamoto et al. 1996), and keratinocytes (Haynes et al. 1997). Fibrillin deposition *in vitro* occurs along tracks carried over from the tissue of origin with a process that is reminiscent of the nucleation of crystals (Brenn et al. 1996). Higher levels of synthesis have been recorded in quiescent postconfluent cells than in actively dividing subconfluent cultures.

We have previously also shown that ECs isolated from bovine large arteries (aorta and pulmonary artery) and the major lymphatic vessel, the thoracic duct, produce fibrillin-1 *in vitro* (Weber et al. 2002, 2004). Fibrillin deposition differs in cultured blood and lymphatic ECs: aortic ECs deposit fibrillin in a honeycomb pattern with fibrillin-free spaces, whereas lymphatic EC cultures form a thick, irregular web of fibrillin in the underlying matrix. Pulmonary artery ECs, which are exposed to the low pressure of pulmonary circulation, have an intermediate arrangement of fibrillin with areas of honeycomb pattern and areas in which fibrillin microfibrils form an irregular web (Weber et al. 2004). These differences in fibrillin deposition correlated with differences in MAGP-1 (Weber et al. 2004): in arterial ECs, MAGP-1 always co-localized with fibrillin. Lymphatic ECs were instead mostly negative for MAGP-1 even at day 4 when fibrillin was abundant throughout the culture. These studies, however, had two limitations: they were performed on bovine, not human ECs, and the cells were isolated from large vessels. The results obtained with lymphatic ECs in particular may not reflect the *in-vivo* situation of initial lymphatic vessels.

Kriehuber et al. (2001) have successfully isolated microvascular lymphatic ECs from human skin by simultaneously exposing the mixed population of cells obtained by the enzymatic digestion of dermis to a serum against podoplanin (specific for lymphatic ECs), an antibody to CD34 (panendothelial) and an antibody to CD45 (for fibroblasts). The cells were then sorted by flow cytometry.

We have isolated lymphatic and blood human dermal microvascular ECs (HDMECs) from human foreskin by the use of D2-40 (Kahn & Marks, 2002), an effective and reliable monoclonal antibody that recognizes podoplanin (Schacht et al. 2005) and specifically binds to lymphatic HDMECs, and verified whether lymphatic and blood HDMECs deposit fibrillin-1 and MAGP-1 *in vitro*. In particular, we wondered whether lymphatic HDMECs deposit MAGP-1 and fibrillin at the same time, like large vessel arterial cells, or whether they deposit fibrillin earlier than MAGP-1 as thoracic duct ECs.

Materials and methods

Isolation and culture of human dermal microvascular endothelial cells

Foreskins were obtained at the Pediatric Surgery Section of the Department of Pediatrics, Obstetrics and Reproductive Medicine of the University of Siena from children (1–5 years old) undergoing circumcision for religious purposes with the informed consent of parents and incubated for 1 h at 37 °C in phosphate-buffered saline (PBS) with penicillin (100 U mL^{-1}; Sigma), streptomycin (100 μg mL^{-1}; Sigma), kanamycin (200 μg mL^{-1}; Sigma), gentamycin (100 μg mL^{-1}; Sigma), and amphotericin B (0.5 μg mL^{-1}; Sigma). Foreskins were then cut in small fragments (2 × 2 mm) and incubated overnight at 4 °C in 3–5 mL of dispase I (2.5 U mL^{-1} PBS; Roche) to facilitate the subsequent separation of the epidermis from the dermis. The epidermis was then peeled off and discarded, and the remaining dermis washed in PBS and incubated for 1 h at 37 °C with 0.25% type 1A collagenase [185 U mL^{-1}; Sigma, in Dulbecco's modified Eagle's medium nutrient mixture F-12 HAM (DME/F-12); Sigma], vigorously shaking the suspension every 30 min. The cell suspension was then diluted with 10 mL of DME/F-12, filtered through a 70-μm nylon mesh and spun. The pellet was resuspended in endothelial growth medium 2-microvascular bullet kit (Bio Whittaker) and seeded into 75-cm^2 gelatin (DIFCO, 0.1% in PBS) coated flasks. At 24 h of seeding, flasks were washed with PBS to remove non-adhering cells and the medium was replaced. At 2–3 days after seeding, cells were trypsinized and separation of HDMECs from contaminating cell types (fibroblasts and smooth muscle cells) was performed with an immunomagnetic procedure using CD31-conjugated microbeads (Miltenyi Biotec) following the manufacturer's instructions. Briefly, the cells were counted and incubated with microbeads for 17 min at 4 °C with a monoclonal antibody to CD31 conjugated with the beads and passed through a magnetic column. $CD31^+$ cells remained in the column. The procedure was repeated until all contaminants were removed and $CD31^+$ cells were seeded on gelatin-coated 75-cm^2 flasks.

As CD31 is a pan-endothelial marker, $CD31^+$ cells are a mixed population of blood and lymphatic HDMECs. The lymphatic-specific monoclonal antibody D2-40 (SIGNET) was therefore used to isolate lymphatic microvascular HDMECs. Prior to incubation with D2-40, the cells were trypsinized, resuspended in DME/F-12 and passed through the column to eliminate $CD31^+$ cells that still had some beads attached. The eluate was spun and resuspended in DME/F-12 with 3% bovine serum albumin (BSA) (Sigma) and D2-40 (final dilution 1 : 20), incubated for 10 min at 4 °C, spun and incubated for 15 min at 4 °C in DME/F-12 containing a rat anti-mouse IgG_1 antibody conjugated with the beads. The cells were passed in the column that this time retained lymphatic HDMECs, which are $CD31^+$ $D2\text{-}40^+$. Blood HDMECs, which are $CD31^+$ $D2\text{-}40^-$, were recovered from the eluate.

The purification steps with CD31 and D2-40 were repeated if necessary.

Cells were seeded on coverslips at a density of 2×10^4 cm^{-2}.

Immunohistochemical characterization of cells

Cells to be tested for the expression of specific markers were seeded onto gelatin-coated round coverslips, allowed to reach confluence and then fixed with cold acetone at −20 °C for 7 min, washed and incubated for 40 min in a solution containing 3% BSA in PBS to block unspecific binding sites. The blood endothelial markers tested were: CD31 (monoclonal, diluted 1 : 20; DAKO), Von Willebrand factor (polyclonal, diluted 1 : 50 after a 2-min permeabilization with 0.2% Triton; DAKO), and CD34 (monoclonal, diluted 1 : 20 after a 2-min permeabilization with 0.2% Triton; Abcam). The lymphatic markers tested were: D2-40 (monoclonal, IgG-1, diluted 1 : 20; SIGNET), Prox-1 (polyclonal, diluted 1 : 250 after a 5-min permeabilization with 0.5% Triton; Acris), Vascular Endothelial Growth Factor Receptor-3 (monoclonal, diluted 1 : 100; Abcam), and LYVE-1 (monoclonal, diluted 1 : 50 after a 2-min permeabilization with 0.2% Triton; LIFESPAN Biosciences). All antibodies were diluted in PBS containing 0.5% BSA (hereafter referred to as buffer). Fluorescein isothiocyanate-labeled goat anti-rabbit or anti-mouse IgG (diluted 1 : 100) or tetramethyl rhodamine isothiocyanate-labeled rabbit anti-mouse IgG (diluted 1 : 200) secondary antibodies (Sigma) were used as appropriate.

Isotypic controls for fibrillin-1 antibody, D2-40, Vascular Endothelial Growth Factor Receptor-3 and LYVE-1 (all IgG_1) were obtained by replacing the primary antibody with monoclonal mouse anti-calbindin-D-28K (vitamin D-dependent calcium-binding protein, IgG_1) anti-bovine (Sigma) and an isotypic control for Prox-1 was obtained by replacing the primary antibody with a rabbit polyclonal antibody anti-calsequestrin-2 (Sigma). Negative controls were also performed by omission of primary antibodies.

Double labeling of fibrillin-1 and microfibril-associated glycoprotein-1

Fibrillin deposition was evaluated on cells grown on gelatine-coated coverslips at confluence and at days 2 and 4 after confluence. Cells were fixed for 7 min in cold acetone, washed and incubated for 40 min in a solution containing 3% BSA in PBS to block unspecific binding sites. The first labeling was performed with an overnight incubation at 4 °C with a polyclonal antibody to MAGP-1 (MFAP-2; Sigma-Aldrich) diluted 1 : 25 in buffer followed by a 90-min incubation with a fluorescein isothiocyanate-conjugated goat anti-rabbit IgG antibody (Sigma) diluted 1 : 100. Unspecific binding sites were again blocked by a 40-min incubation with PBS containing 3% BSA. After washing, cells were incubated for 2 h with a monoclonal antibody to fibrillin-1 (Chemicon) diluted 1 : 100 in buffer. The reaction was revealed with a 90-min incubation with the secondary antibody (tetramethyl rhodamine isothiocyanate-conjugated goat anti-mouse IgG; DAKO) diluted 1 : 200 in buffer. After washing, coverslips were mounted upside down on glass slides with DABCO mounting medium (Sigma).

Morphometric analysis of fibrillin deposition

Fibrillin deposition was recorded at confluence (day 0) and at day 2 and 4 after confluence. Coverslips with adhering cells were photographed in randomly selected fields with a ×40 objective, taking care to maintain fixed exposure parameters. Fibrillin deposition was evaluated with a morphometric program, NIS Elements (Nikon), on at least 50 photographs per condition, measuring the mean length of fibrillin fibers per photographic field, the mean number of branching points per photographic field and the amount of fibrillin deposited expressed as sum density after selecting the proper threshold. The sum density is the sum

of individual optical densities (ODs) of each pixel in the area being measured. The OD is evaluated according to the formula:

$$\text{O.D.} = -\log(\text{Pixel Intensity value} + 0.5)/62.5.$$

Statistical analysis was performed using Linear Mixed Models (package LMER of R, http://www.r-project.org), including a variable for each single experiment as a factor with random effects. Natural log transformation was used to decrease variance heterogeneity. A value of $P < 0.05$ for a two-tails distribution was considered significant.

Results

Phase contrast microscopy

The initial digest of human foreskin dermis with collagenase yielded a mixed population of HDMECs and contaminants, mainly smooth muscle cells and fibroblasts (Fig. 1A). After purification with CD31, isolated groups of HDMECs, recognizable by their polygonal shape, were evident (Fig. 1B). These cells proliferated and reached confluence in 3–6 days. At this time, separation of lymphatic and blood HDMECs was attained with D2-40. The latter constituted approximately 30% of the total CD31-positive population. Lymphatic and blood HDMECs at confluence displayed a typical cobblestone morphology (Fig. 1C,D) and contained approximately 4.5×10^4 cells cm^{-2}. As ECs are contact inhibited, this number did not significantly increase at days 2 and 4 after confluence.

Characterization

More than 95% of blood HDMECs ($CD31^+$ $D2\text{-}40^-$) were intensely labeled by all blood endothelial markers tested and by the pan-endothelial marker CD31 (Fig. 2). CD31 stained cell borders, whereas the fluorescence of Von Willebrand factor was in the cytoplasm and had a punctate appearance and that of the transmembrane glycoprotein CD34, also punctate, was particularly evident in the perinuclear region.

More than 90% of lymphatic HDMECs ($CD31^+$ $D2\text{-}40^+$) were intensely labeled by all lymphatic markers tested and by the pan-endothelial marker CD31 (Fig. 3). CD31 and D2-40 mainly stained cell borders, whereas the fluorescence of LYVE-1 and Vascular Endothelial Growth Factor Receptor-3 was scattered all over the cell membrane and had a punctate appearance. Prox-1 typically stained cell nuclei.

Fibrillin-1 deposition by blood human dermal microvascular endothelial cells

Fibrillin was initially deposited as short, thin strands that gradually united to form linear arrays. These arranged in a wide-mesh honeycomb pattern (Pattern A, Fig. 4A). HDMECs were visible in the large fibrillin-free spaces of the honeycomb surrounded by fibrillin strands. This initial wide-mesh honeycomb was subsequently modified by thin strands of fibrillin arising from the honeycomb borders and subdividing the fibrillin-free spaces into smaller ones. At the same time, the space between different honeycombs was also filled by a thin net of fibrillin fibers in which some small honeycombs formed (Pattern B, Fig. 4B). Fibrillin-free spaces were gradually filled until an almost continuous net of fibrillin was formed under the cell layer with some of the original honeycomb pattern still recognizable (Pattern C, Fig. 4C). Fibrillin eventually formed an almost continuous network with an uneven thickness, large strands of fibrillin co-existing with a mesh of thin fibers (Pattern D, Fig. 4D). Different patterns co-existed in the same culture, 'hot spots'

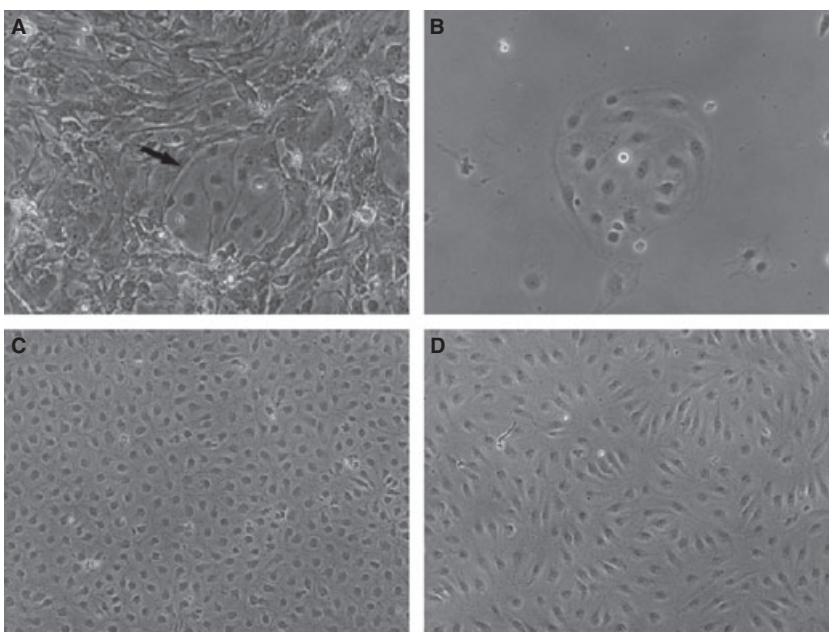

Fig. 1 Phase contrast microscopy of human dermal microvascular endothelial cells (HDMECs). (A) Prior to purification, contaminants constitute the majority of the obtained cell population. Arrow indicates a group of HDMECs. (B) An isolated group of HDMECs after purification with CD31. The cells have a polygonal shape. Typical cobblestone morphology at confluence of blood (C) and lymphatic (D) HDMECs after separation of lymphatic HDMECs from the bulk of $CD31^+$ cells with D2-40. Original magnifications: A and B, ×20; C and D, ×10.

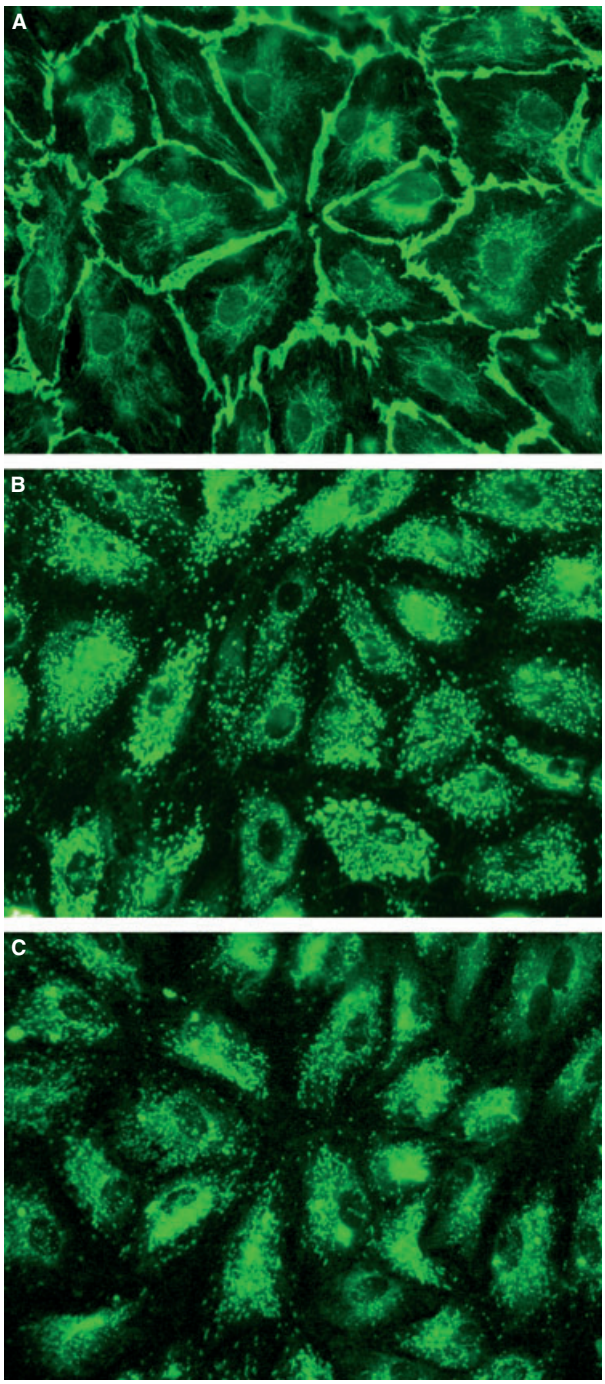

Fig. 2 Characterization of blood microvascular human dermal microvascular endothelial cells. Cell borders are stained by the pan-endothelial marker CD31 (A), whereas the fluorescence of Von Willebrand factor (B) and CD34 (C) is scattered all over the cell and has a punctate appearance. Original magnification ×40.

(Patterns C and D) probably corresponding to the initial tracks carried over from the vessel of origin.

As shown in Figure 5(A), Pattern A prevailed in confluent cultures and progressively decreased at days 2 and 4; Pattern B increased from confluence to day 2 and subsequently decreased in concomitance with the increase of Pattern C at day 4. Pattern D was negligible at confluence and day 2 and increased to 11.4% of cases at day 4. Overall, there was a gradual shift to more complex patterns with time in culture.

Fibrillin-1 deposition by lymphatic human dermal microvascular endothelial cells

Fibrillin deposition by lymphatic HDMECs occurred with the same patterns described for blood HDMECs. Moreover, two additional initial patterns were observed as an alternative to Patterns A and B: Pattern α in which fibrillin formed a dense mesh of short segments (Fig. 4E) that gradually united in longer filaments arranged in semicircular arrays (Pattern β, Fig. 4F). The fibrillin mesh became gradually denser and Patterns C and D were clearly recognizable at more advanced stages of deposition.

Different patterns of deposition were detected in the same glass coverslips (Fig. 5B). Pattern A prevailed at confluence, decreasing at days 2 and 4 parallel to the linear increase of Patterns B and C. Pattern D, which was absent at confluence, increased to 6.1% at day 4. Patterns α and β decreased gradually from confluence to day 4.

A schematic drawing summarizing fibrillin deposition patterns in blood and lymphatic ECs is provided in Fig. 6.

Microfibril-associated glycoprotein-1 deposition by blood and lymphatic human dermal microvascular endothelial cells

Both blood and lymphatic HDMECs had already deposited MAGP-1 in the underlying matrix at confluence. MAGP-1 perfectly co-localized with fibrillin-1 in all blood (Fig. 7A–D) and lymphatic (Fig. 7E–H) HDMEC cultures at all times tested.

Quantitative analysis

The area covered by fibrillin, visually evaluated by two different independent observers (E.G. and M.V.), was approximately 25% at confluence, 60% at day 2 and 80% at day 4 after confluence in blood HDMECs, and approximately 60% at confluence, 65% at day 2 and 70% at day 4 after confluence in lymphatic HDMECs.

Blood and lymphatic HDMECs expressed, at confluence, a constitutive level of fibrillin, which significantly increased over time in both cell types (Fig. 8). At confluence, fibrillin deposition was slightly greater in lymphatic (log OD 12.6 ± 0.2) than in blood (11.6 ± 0.5, $P = 0.033$) HDMECs; however, the increase over time in the log-transformed OD was significantly steeper in blood HDMECs (0.52 ± 0.11 vs. 0.18 ± 0.07 per day, $P = 0.013$), and the levels at day 4 were superimposable. When converted back to base 10 numbers, these data indicate that fibrillin OD increased by an average

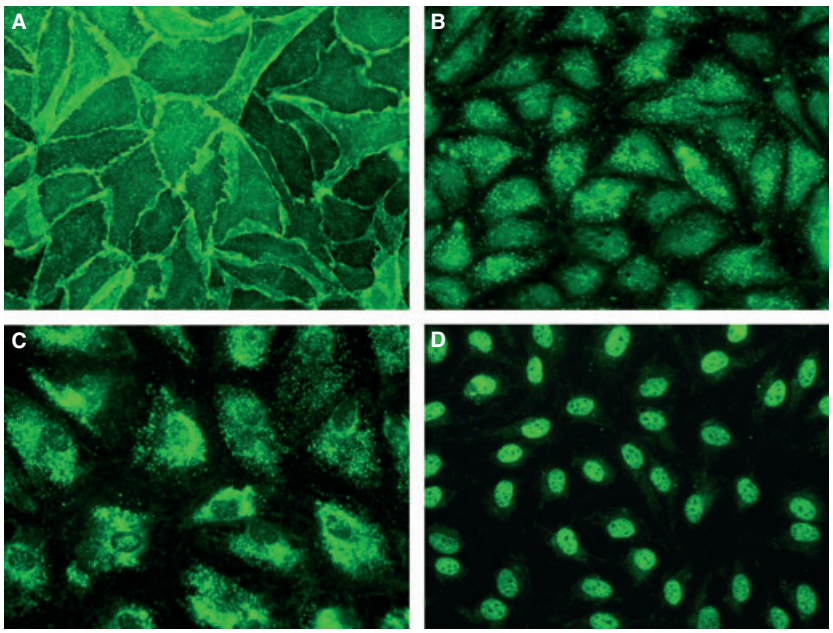

Fig. 3 Characterization of lymphatic microvascular human dermal microvascular endothelial cells. Cell borders are stained by D2-40 (A), whereas the fluorescence of Vascular Endothelial Growth Factor Receptor-3 (B) and LYVE-1 (C) is in the cytoplasm and has a punctate appearance. Prox-1 (D) labels nuclei. Original magnification ×40.

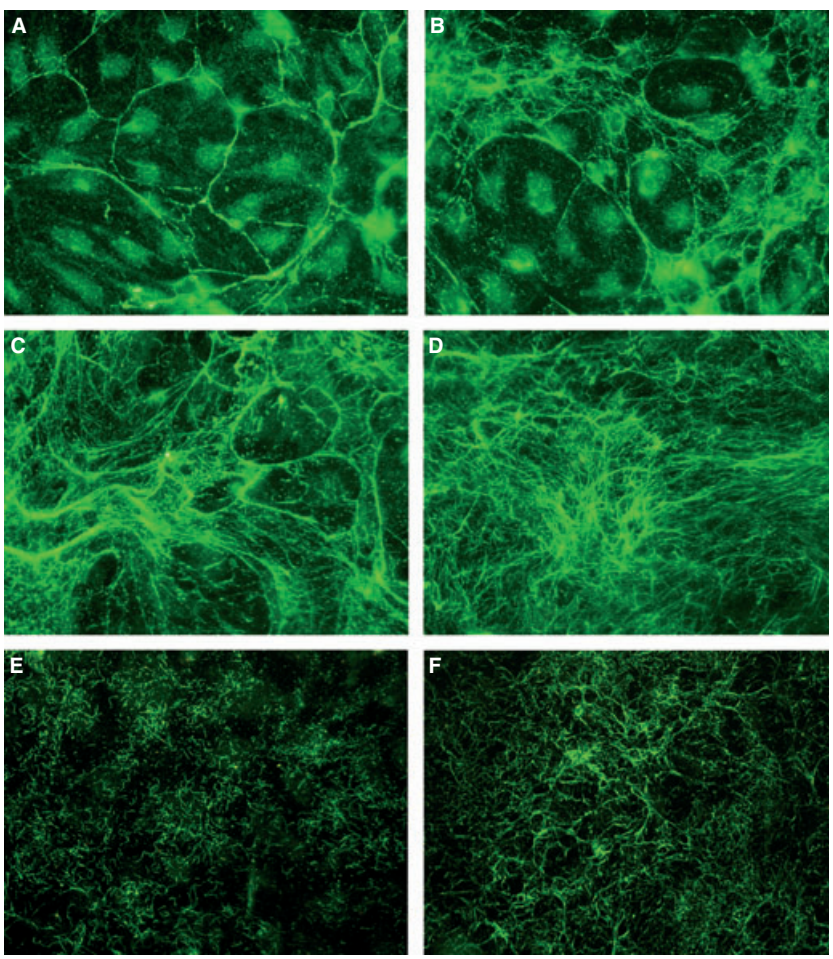

Fig. 4 Fibrillin deposition patterns. (A) Pattern A: wide-mesh honeycomb pattern. Human dermal microvascular endothelial cells (HDMECs) are visible in the large fibrillin-free spaces. (B) Pattern B: thin strands of fibrillin arising from the honeycomb borders subdivide fibrillin-free spaces into smaller ones. The space between different honeycombs is also filled by a thin net of fibrillin fibers. (C) Pattern C: the wide honeycomb mesh spaces are filled by an almost continuous net of fibrillin. Some of the original honeycomb pattern is still recognizable. (D) Pattern D: fibrillin forms an almost continuous network with an uneven thickness. The honeycomb is no longer recognizable. (E) and (F) Alternative fibrillin deposition patterns in lymphatic HDMECs. (E) Pattern α: thin short strands of fibrillin form a dense mesh. (F) Pattern β: fibrillin strands unite in longer filaments that arrange in semicircular arrays. Original magnification ×40.

of 68% (95% confidence interval 34–111%) per day in blood and by 20% per day (95% confidence interval 4–38%) in lymphatic HDMECs.

The morphometric evaluation of the complexity of fibrillin deposition by blood and lymphatic HDMECs in the different patterns was performed by measuring the mean OD,

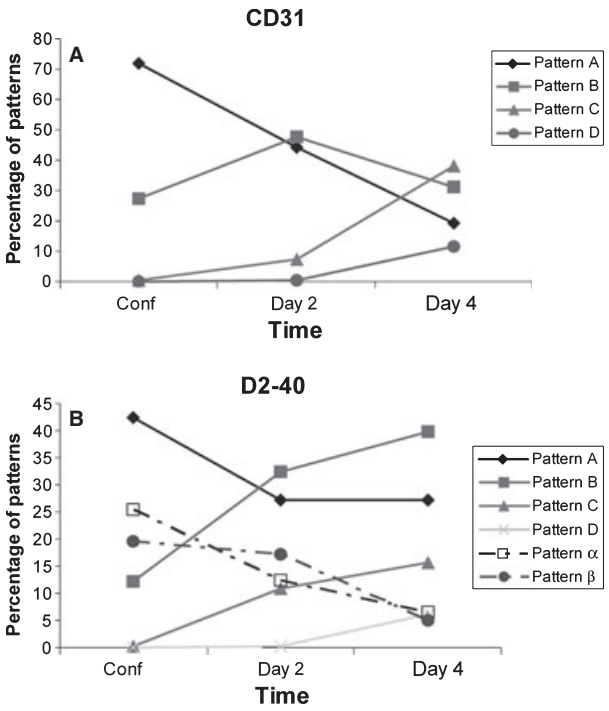

Fig. 5 Percentage of different patterns of fibrillin deposition. (A) Blood and (B) lymphatic human dermal microvascular endothelial cells (HDMECs) at confluence and at days 2 and 4 after confluence. Overall, in blood HDMECs (A), there is a decrease of the simplest Pattern A and an increase of the more complex ones (Patterns B, C and D) with time in culture. In lymphatic HDMECs (B), Pattern A prevails at confluence and decreases at day 2; Patterns B and C increase linearly with time; and Pattern D, absent at confluence, is 6.1% at day 4. Pattern α decreases gradually with time, whereas Pattern β decreases mainly from day 2 to day 4.

mean length of fibrillin fibers, and mean number of branching points per photographic field. Values are reported in Table 1. Overall, these parameters progressively increased from Pattern A to Pattern D.

Discussion

This is, to our knowledge, the first report that human cultured blood and lymphatic microvascular ECs deposit fibrillin in the underlying matrix. In both cell types, fibrillin was deposited with different patterns co-existing in the same culture, probably due to different amounts of fibrillin carried over from the vessel of origin (Brenn et al. 1996). As the percentage of Patterns A and B gradually decreased from confluence to days 2 and 4 while Patterns C and D increased at the same time, we propose that Pattern A may represent an early stage of deposition and that a progressive shift from the simplest Pattern A to the most complex Pattern D occurs with time in culture.

Blood HDMECs deposited fibrillin in a honeycomb pattern, similarly to ECs obtained from bovine large arteries (Weber et al. 2004) and auricular chondrocytes (Brown-Augsburger et al. 1996). Lymphatic HDMECs, at variance with bovine thoracic duct ECs (Weber et al. 2004), behaved similarly to their blood counterparts.

Overall, as particularly demonstrated by patterns α and β, fibrillin was more finely and uniformly distributed and more abundant at confluence in lymphatic than in blood HDMECs. This could be the result of a more diffuse carrying over from the vessel of origin, fibrillin microfibrils probably corresponding to anchoring filaments that are present in all lymphatic ECs. Fibrillin deposition in the underlying extracellular matrix, representing a specific need of the lymphatic initial vessel rather than of the surrounding tissue, would, however, increase moderately with time. An opposite trend was observed in blood HDMECs that had less fibrillin at confluence but produced progressively much more fibrillin with time in culture. Their steep increase in fibrillin deposition may indicate that blood microvascular ECs in general have an intrinsic potential to produce large amounts of fibrillin when required.

As to the fact that lymphatic HDMECs behave like their blood counterparts rather than like lymphatic ECs isolated from the thoracic duct in terms of deposition of fibrillin, we believe that this may be due to differences in MAGP-1 expression by the two cell types. We have previously postulated that a honeycomb pattern is formed *in vitro* only when fibrillin-1 and MAGP-1 are both already expressed at confluence. In the absence of MAGP-1, as in thoracic duct ECs, fibrillin is deposited in an irregular web. We report

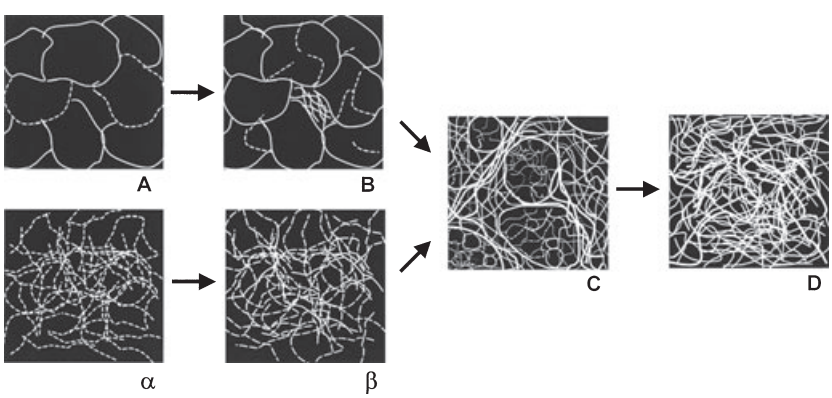

Fig. 6 Scheme of fibrillin deposition patterns. Schematic drawing representing fibrillin deposition by blood and lymphatic human dermal microvascular endothelial cells in culture. The two alternative routes of fibrillin deposition merge in Pattern C.

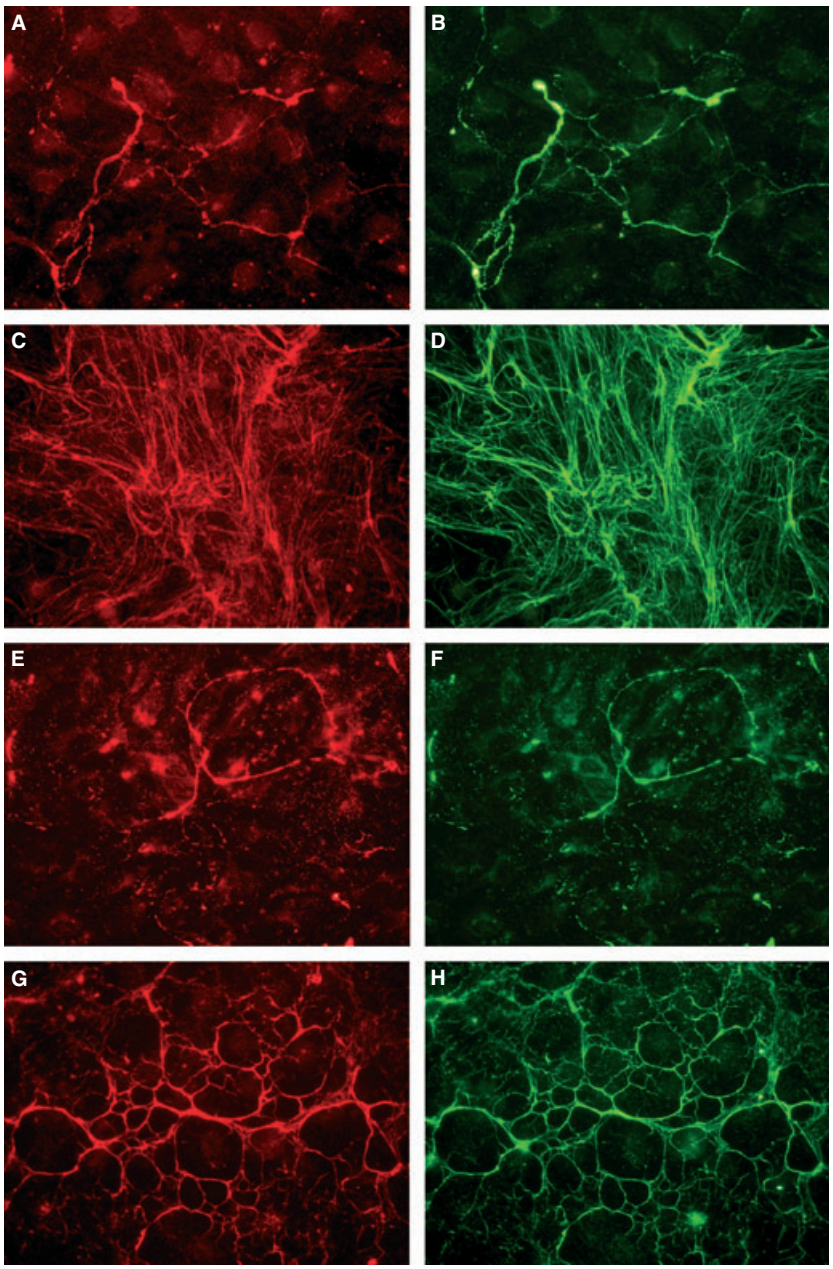

Fig. 7 Co-localization of fibrillin and microfibril-associated glycoprotein (MAGP)-1. Fibrillin (left) and MAGP-1 (right) in blood (A–D) and lymphatic (E–H) human dermal microvascular endothelial cells at days 2 (A,B,E,F) and 4 (C,D,G,H) after confluence. Original magnification ×40.

here that MAGP-1 co-localized with fibrillin not only in blood but also in lymphatic HDMECs from the very first time-point assayed. Our present data thus bring support to the hypothesis that MAGP-1 expression is related to the formation of a honeycomb pattern. Similar results have been reported for cultured auricular chondrocytes in which fibrillin, MAGP, and tropoelastin co-localize in a honeycomb network (Brown-Augsburger et al. 1996).

Other possible explanations for the discrepancy between our previous data on thoracic duct ECs and the present findings obtained with lymphatic HDMECs are species differences (human vs. bovine) or differences in the vessel of origin (microvessels vs. large vessels). The thoracic duct wall contains smooth muscle cells and fibroblasts, which also produce fibrillin, whereas initial lymphatic vessels are made solely by the endothelium. Thus, all of the fibrillin microfibrils associated with initial lymphatic vessels are probably produced by lymphatic endothelium. Cultured lymphatic HDMECs would retain the capability to produce the anchoring filaments that they need for their physiological activity of draining interstitial fluids and macromolecules.

Fibrillin has a key role in constituting a track for elastin deposition. Elastic fibers confer mechanical resilience to the skin, which needs to be able to return to its initial shape after deformation or distortion (Ryan, 1995). In the

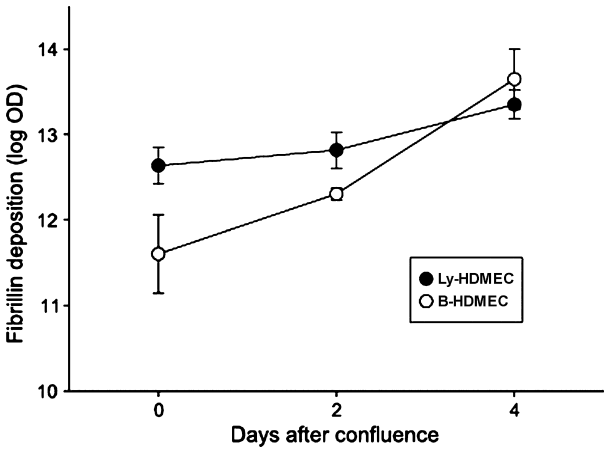

Fig. 8 Quantification of fibrillin deposition. Sum density of fibrillin in blood and lymphatic human dermal microvascular endothelial cells (HDMECs) at confluence and at days 2 and 4 after confluence. At confluence, fibrillin deposition was greater in lymphatic (Ly-HDMEC) than in blood (B-HDMEC) HDMECs but, as fibrillin increase was significantly steeper in blood HDMECs, at day 4 fibrillin levels were superimposable in the two cell types.

Table 1 Morphometric evaluation of fibrillin deposition by blood and lymphatic human dermal microvascular endothelial cells (HDMECs) in the different patterns.

HDMECs	Optical density per field		Fiber length (μm) per field		Branching points per field	
Blood						
Pattern A	11.69	± 0.22	45	(40–51)	30	(20–43)
Pattern B	13.01	± 0.23	74	(67–83)	67	(57–79)
Pattern C	14.25	± 0.23	122	(107–138)	131	(109–158)
Pattern D	14.88	± 0.1	174	(159–190)	261	(203–335)
Lymphatic						
Pattern A	12.1	± 0.14	21	(17–26)	15	(11–19)
Pattern B	13.07	± 0.12	40	(36–45)	37	(30–44)
Pattern C	14.42	± 0.15	95	(84–108)	147	(125–174)
Pattern D	14.76	± 0.13	187	(173–202)	388	(316–476)
Pattern α	13.13	± 0.11	12	(10–15)		
Pattern β	13.28	± 0.07	29	(26–32)		

Geometric mean ± SE for optical density, geometric mean with 95% confidence interval in parenthesis for fiber length and branching points. Fiber length and branching points increase from Pattern A to D in both blood and lymphatic HDMECs. Mean fiber length is smaller in lymphatic than in blood HDMECs except for Pattern D. No branching points were detected in Patterns α and β.

regenerating skin of burned children, fibrillin microfibrils have been shown to precede and guide elastin deposition (Raghunath et al. 1996). Given the strategic importance of fibrillin in the skin under normal conditions and during skin repair, it makes sense that several cell types contribute to its production: keratinocytes (Haynes et al. 1997) probably account for fibrillin deposition at the dermo-epidermal junction, whereas fibroblasts (Sakai et al. 1986; Kielty & Shuttleworth, 1993) and, based on the present report, also blood and lymphatic ECs may be responsible for fibrillin and hence elastin deposition in the remainder of the dermis.

Acknowledgements

The authors wish to thank Prof. R. Gerli for helpful discussions and Prof. P. Sestini for statistical evaluation of the data. This work was supported by the University of Siena (Progetto di Ateneo per la Ricerca).

References

Brenn T, Aoyama T, Francke U, et al. (1996) Dermal fibroblast culture as a model system for studies of fibrillin assembly and pathogenetic mechanisms: defects in distinct groups of individuals with Marfan's syndrome. *Lab Invest* **75**, 389–402.

Brown-Augsburger P, Broekelmann T, Mecham L, et al. (1994) Microfibril-associated glycoprotein binds to the carboxyl-terminal domain of tropoelastin and is a substrate for transglutaminase. *J Biol Chem* **269**, 28443–28449.

Brown-Augsburger P, Broekelmann T, Rosenbloom J, et al. (1996) Functional domains on elastin and microfibril-associated glycoprotein involved in elastic fibre assembly. *Biochem J* **318**, 149–155.

Carta L, Pereira L, Arteaga-Solis E, et al. (2006) Fibrillins 1 and 2 perform partially overlapping functions during aortic development. *J Biol Chem* **281**, 8016–8023.

Casley-Smith JR (1980) Are the initial lymphatics normally pulled open by the anchoring filaments? *Lymphology* **13**, 120–129.

Dubuisson L, Lepreux S, Bioulac-Sage P, et al. (2001) Expression and cellular localization of fibrillin-1 in normal and pathological human liver. *J Hepatol* **34**, 514–522.

Gerli R, Ibba L, Fruschelli C (1990) A fibrillar elastic apparatus around human lymph capillaries. *Anat Embryol* **181**, 281–286.

Gibson MA, Finnis ML, Kumaratilake JS, et al. (1998) Microfibril-associated glycoprotein-2 (MAGP-2) is specifically associated with fibrillin-containing microfibrils but exhibits more restricted patterns of tissue localization and developmental expression than its structural relative MAGP-1. *J Histochem Cytochem* **46**, 871–886.

Haynes SL, Shuttleworth CA, Kielty CM (1997) Keratinocytes express fibrillin and assemble microfibrils: implications for dermal matrix organization. *Br J Dermatol* **137**, 17–23.

Henderson M, Polewski R, Fanning JC, et al. (1996) Microfibril-associated glycoprotein-1 (MAGP-1) is specifically located on the beads of the beaded-filament structure for fibrillin-containing microfibrils as visualized by the rotary shadowing technique. *J Histochem Cytochem* **44**, 1389–1397.

Jurisic G, Detmar M (2009) Lymphatic endothelium in health and disease. *Cell Tissue Res* **335**, 97–108.

Kahn HJ, Marks A (2002) A new monoclonal antibody, D2-40, for detection of lymphatic invasion in primary tumors. *Lab Invest* **82**, 1255–1257.

Kielty CM, Shuttleworth CA (1993) Synthesis and assembly of fibrillin by fibroblasts and smooth muscle cells. *J Cell Sci* **106**, 167–173.

Kitahama S, Gibson MA, Hatzinikolas G, et al. (2000) Expression of fibrillins and other microfibril-associated proteins in human bone and osteoblast-like cells. *Bone* **27**, 61–67.

Kriehuber E, Breiteneder-Geleff S, Groeger M, et al. (2001) Isolation and characterization of dermal lymphatic and blood endothelial cells reveal stable and functionally specialized cell lineages. *J Exp Med* **194**, 797–808.

Lee B, Godfrey M, Vitale E, et al. (1991) Linkage of Marfan syndrome and a phenotypically related disorder to two different fibrillin genes. *Nature* **352**, 330–334.

Lemaire R, Bayle J, Mecham RP, et al. (2007) Microfibril-associated MAGP-2 stimulates elastic fiber assembly. *J Biol Chem* **282**, 800–808.

Raghunath M, Bächi T, Meuli M, et al. (1996) Fibrillin and elastin expression in skin regenerating from cultured keratinocyte autografts: morphogenesis of microfibrils begins at the dermo-epidermal junction and precedes elastic fiber formation. *J Invest Dermatol* **106**, 1090–1095.

Ramirez F (2000) Pathophysiology of the microfibril/elastic fiber system: introduction. *Matrix Biol* **19**, 455–456.

Ramirez F, Sakai LY (2010) Biogenesis and function of fibrillin assemblies. *Cell Tissue Res* **339**, 71–82.

Robinson PN, Arteaga-Solis E, Baldock C, et al. (2006) The molecular genetics of Marfan syndrome and related disorders. *J Med Genet* **43**, 769–787.

Rossi A, Weber E, Sacchi G, et al. (2007) Mechanotransduction in lymphatic endothelial cells. *Lymphology* **40**, 102–113.

Ryan TJ (1995) Mechanical resilience of skin: a function of blood supply and lymphatic drainage. *Clin Dermatol* **13**, 429–432.

Ryan TJ (2009) Elephantiasis, elastin, and chronic wound healing: 19th century and contemporary viewpoints relevant to hypotheses concerning lymphedema, leprosy, erysipelas, and psoriasis – review and reflections. *Lymphology* **42**, 19–25.

Sakai LY, Keene DR, Engvall E (1986) Fibrillin, a new 350-kD glycoprotein, is a component of extracellular microfibrils. *J Cell Biol* **103**, 2499–2509.

Sakamoto H, Broekelmann T, Cheresh DA, et al. (1996) Cell-type specific recognition of RGD- and non-RGD-containing cell binding domains in fibrillin-1. *Biol Chem* **271**, 4916–4922.

Scavelli C, Weber E, Aglianò M, et al. (2004) Lymphatics at the crossroads of angiogenesis and lymphangiogenesis. *J Anat* **204**, 433–449.

Schacht V, Dadras SS, Johnson LA, et al. (2005) Up-regulation of the lymphatic marker podoplanin, a mucin-type transmembrane glycoprotein, in human squamous cell carcinomas and germ cell tumors. *Am J Pathol* **166**, 913–921.

Solito R, Alessandrini C, Fruschelli M, et al. (1997) An immunological correlation between the anchoring filaments of initial lymph vessels and the neighboring elastic fibers: a unified morphofunctional concept. *Lymphology* **30**, 194–202.

Stephan S, Ball SG, Williamson M, et al. (2006) Cell-matrix biology in vascular tissue engineering. *J Anat* **209**, 495–502.

Wagenseil JE, Mecham RP (2007) New insights into elastic fiber assembly. *Birth Defects Res C Embryo Today* **81**, 229–240.

Weber E, Rossi A, Solito R, et al. (2002) Focal adhesion molecules expression and fibrillin deposition by lymphatic and blood vessel endothelial cells in culture. *Microvasc Res* **64**, 47–55.

Weber E, Rossi A, Solito R, et al. (2004) The pattern of fibrillin deposition correlates with microfibril-associated glycoprotein 1 (MAGP-1) expression in cultured blood and lymphatic endothelial cells. *Lymphology* **37**, 116–126.